

## Numerical Study of Mixed Convection Flow inside Ventilated Enclosure by Finite Volume Method

Robins Aikkara<sup>1</sup>, Aboobacker Kadengal<sup>2</sup>

<sup>1</sup>Department of Mechanical Engineering, LBS College of Engineering, Kasaragod, India

<sup>2</sup>Department of Mechanical Engineering, LBS College of Engineering, Kasaragod, India

**Abstract:** *Mixed convection from a uniform heat source on the top wall of a enclosure with different inlet and outlet opening is studied numerically. Two-dimensional forms of non-dimensional Navier-Stokes equations are solved by using control volume based finite volume technique. Three typical values of the Reynolds numbers are chosen as  $Re = 1, 10,$  and  $100$  and steady, laminar results are obtained in the values of Richardson number as  $Ri = 0, 1$  and  $10$  and the values of Prandtl numbers as  $Pr = 0.1, 0.71, 1$  and  $10$ . The parametric studies for a wide range of governing parameters show consistent performance of the present numerical approach to obtain as stream functions and temperature profiles. Heat transfer rates at the heated walls are presented based on the value of  $Re$  and  $Pr$ . The computational results indicate that the heat transfer is strongly affected by Reynolds number and Richardson number. In the present investigation, bottom wall is uniformly heated while the two vertical walls are maintained at constant cold temperature and the top wall is well insulated. A complete study on the effect of  $Ri$  shows that the strength of circulation increases with the increase in the value of  $Ri$  irrespective of  $Re$  and  $Pr$ . As the value of  $Ri$  increases, there occurs a transition from conduction to convection dominated flow at  $Ri = 1$ . A detailed analysis of flow pattern shows that the natural or forced convection is based on both the parameters  $Ri$  and  $Pr$ .*

**Keywords:** *Mixed convection; Ventilated enclosure; Uniform heating; Reynolds number; Richardson number and Prandtl number.*

### 1. INTRODUCTION

In a mixed convection, both natural convection and forced convection participate in the heat transfer process. The bulk fluid flow direction can be any of the three possible directions in a horizontal channel, forward, backward or upward. The forced flow can be in the same direction as the flow created by natural convection, and this flow condition is called assisting mixed convection. Whereas, for the other case, forced flow direction is in an opposing direction to the flow that is created by buoyancy, and this flow condition is referred to as opposing mixed convection.

Since the early work by Burggraf [1], the lid-driven cavity flow is considered as the classical test problem for the assessment of numerical methods and the validation of Navier-Stokes codes. Highly-accurate solutions for the lid-driven cavity flow are computed by a Chebyshev collocation method is done by O. Botella [2]. Accuracy of the solution is achieved by using a subtraction method of the leading terms of the asymptotic expansion of the solution of the Navier-Stokes equations in the vicinity of the corners, where the velocity is discontinuous. Critical comparison with former numerical experiments confirms the high-accuracy of the method, and extensive results for the flow at Reynolds number  $Re = 1000$  are presented. The Charles-Henri Bruneau [3], numerically simulate of the 2D lid-driven cavity flow are performed for a wide range of Reynolds numbers. Accurate benchmark results are provided for steady solutions as well as for periodic solutions around the critical Reynolds number.

A brief literature review shows that the case with enclosures having openings using forced, natural, mixed convection and conduction has been studied in a few cases. The most noted study was by Chen et al. [4]. The purpose of their work was to obtain convective heat transfer coefficients for a ventilated room with mixed convection (laminar and turbulent flows) for a relatively low Reynolds number when the boundary layers are not fully developed. The experiments that were carried out in a  $5.6 \times 3.0 \times 3.2$  m high chamber concerned the measurements of enclosure surface temperatures, air temperature differences between the enclosure surfaces and the air points 100 mm from the surfaces, the total heat fluxes through the surfaces and the air velocity 100 mm from the surface.

In the present investigation, top wall is uniformly heated while the two vertical walls are maintained at constant cold temperature and the bottom wall is well insulated. The inlet openings are located at the top of left and right vertical walls and outlet openings are located at bottom of right and left vertical walls. A complete study on the effect of Gr shows that the strength of circulation increases with the increase in the value of Ri irrespective of Re and Pr. As the value of Ri increases, there occurs a transition from conduction to convection dominated flow. A detailed analysis of flow pattern shows that the natural or forced convection is based on both the parameters Ri and Pr.

## 2. MATHEMATICAL FORMULATION

A two-dimensional ventilated enclosure is considered for the present study with the physical dimension as shown in Fig.1. The ventilated enclosure with two inlet openings located on the top of both vertical walls; the outlet openings on the bottom of both vertical walls; and constant wall temperature heat source on the top wall. In this case model is two-dimensional, because of depth is infinitely long. The width of the all openings is kept same and equal to one fourth of vertical wall. We all ready seen that bottom wall of enclosure is taken as adiabatic. The flow velocities of the fluid through the inlet opening are assumed to be uniform ( $U_0$ ) at constant temperature  $T_c$ . The flow is assumed to be laminar and the fluid properties are assumed to be constant except for the density variation which is modeled according to Boussinesq approximation while viscous dissipation effects are considered to be negligible. The viscous incompressible flow and the temperature distribution inside the cavity are governed by the Navier–Stokes and the energy equations, respectively. The aim of the current work is to investigate the steady state solutions and hence, we have considered the time independent differential governing equations. Similar procedure was also followed in the recent work on mixed convection. A number of earlier works was based on steady state solutions which were obtained via steady mathematical model. The governing equations are non-dimensionalized to yield

$$\frac{\partial U}{\partial X} + \frac{\partial V}{\partial Y} = 0 \tag{1}$$

$$U \frac{\partial U}{\partial X} + V \frac{\partial U}{\partial Y} = -\frac{\partial P}{\partial X} + \frac{1}{Re} \left( \frac{\partial^2 U}{\partial X^2} + \frac{\partial^2 U}{\partial Y^2} \right) \tag{2}$$

$$U \frac{\partial V}{\partial X} + V \frac{\partial V}{\partial Y} = -\frac{\partial P}{\partial Y} + \frac{1}{Re} \left( \frac{\partial^2 V}{\partial X^2} + \frac{\partial^2 V}{\partial Y^2} \right) + \frac{Gr}{Re^2} \theta \tag{3}$$

$$U \frac{\partial \theta}{\partial X} + V \frac{\partial \theta}{\partial Y} = \frac{1}{RePr} \left( \frac{\partial^2 \theta}{\partial X^2} + \frac{\partial^2 \theta}{\partial Y^2} \right) \tag{4}$$

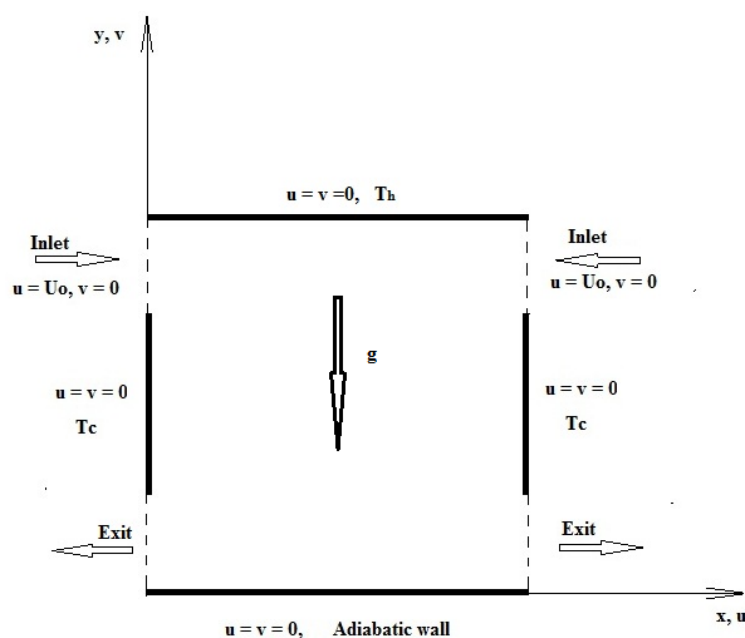


Fig1. Schematic diagram of a physical system

The transformed boundary conditions are:

$$U(X, 1) = 1,$$

$$U(X, 0) = U(0, Y) = U(1, Y) = 0$$

$$V(X, 0) = V(X, 1) = V(0, Y) = V(1, Y) = 0$$

$$\theta(X, 0) = 1$$

$$\theta(0, Y) = \theta(1, Y) = 0$$

$$\frac{\partial \theta}{\partial Y}(X, 1) = 0$$

The dimensionless variables and parameters are defined as follows:

$$X = \frac{x}{L}, Y = \frac{y}{L}, U = \frac{u}{U_0}$$

$$V = \frac{v}{V_0}, \theta = \frac{T - T_c}{T_h - T_c}, P = \frac{p}{\rho U_0^2}$$

$$Pr = \frac{\nu}{\alpha}, Re = \frac{U_0 L}{\nu}, Gr = \frac{g \beta (T_h - T_c) L^3}{\nu^2}$$

Here  $x$  and  $y$  are the distances measured along the horizontal and vertical directions, respectively;  $u$  and  $v$  are the velocity components in  $x$  and  $y$  directions, respectively;  $T$  denotes the temperature;  $p$  is the pressure and  $\rho$  is the density;  $T_h$  and  $T_c$  are the temperature at the hot and cold walls, respectively;  $L$  is the length of the side of the ventilated cavity;  $X$  and  $Y$  are dimensionless coordinates varying along horizontal and vertical directions, respectively;  $U_0$  is the velocity of the upper wall;  $U$  and  $V$  are dimensionless velocity components in the  $X$  and  $Y$  directions, respectively;  $\theta$  is the dimensionless temperature;  $P$  is the dimensionless pressure;  $Gr$ ,  $Re$  and  $Pr$  are Grashof, Reynolds and Prandtl number, respectively.

### 3. SOLUTION METHODOLOGY

The momentum and energy balance equations [Eqs. (2) – (4)] are the combinations of a system of equations which have been solved using the finite volume method. The continuity equation [Eq. (1)] has been used as a constraint due to mass conservation and this constraint may be used to obtain the pressure distribution. In order to solve Eqs. (2) – (3), we use the finite volume discretisation procedure, if the nonlinearity in the momentum equations appears to be a difficulty in iteration procedure. Starting with a guessed velocity field, we could iteratively solve the momentum equations to arrive at the converged solution for the velocity components. The real difficulty in the calculation of the velocity field lies in the unknown pressure field. The pressure gradient forms a part of the source term for a momentum equation. For a given pressure field, there is no particular difficulty in solving the momentum equation. The pressure field is indirectly specified via the continuity equation [Eq. (1)]. When the correct pressure field is substituted into the momentum equations, the resulting velocity field satisfies the continuity equation.

The discretised form of X-momentum [Eq. (2)] is written as

$$a_e U_e = \sum a_{nb} U_{nb} + b + (P_p - P_e) A_e \quad (5)$$

Where  $A_e = \Delta Y$

The discretised form of Y-momentum [Eq. (3)] is written as

$$a_n V_n = \sum a_{nb} V_{nb} + b + (P_p - P_n) A_n \quad (6)$$

Where  $A_n = \Delta X$ .

The momentum equations can be solved only when the pressure field is given. Unless the correct pressure field is employed the resulting velocity field will not satisfy the continuity equations. Such an imperfect velocity field based on a guessed pressure field  $P^*$  will be denoted by  $U^*$ ,  $V^*$ . This “starred” velocity field will result from the solution of the following discretisation equations:

$$a_{\varepsilon}U^*_{\varepsilon} = \sum a_{nb}U^*_{nb} + b + (P^*_P - P^*_E)A_{\varepsilon} \quad (7)$$

$$a_nV^*_n = \sum a_{nb}V^*_{nb} + b + (P^*_P - P^*_N)A_n \quad (8)$$

In these equations [Eq. (7), (8)], the velocity components and pressure have been given the superscript\*.

The guessed pressure  $P^*$  and resulting starred velocity field will progressively get closer to satisfying the continuity equation. Let us propose that the correct pressure  $P$  is obtained from

$$P = P^* + P' \quad (9)$$

Where will be called the pressure correction. The corresponding velocity corrections can be introduced in a similar manner:

$$U = U^* + U', V = V^* + V' \quad (10)$$

The equation (12) will be used to correct the momentum equations:

$$U_{\varepsilon} = U^*_{\varepsilon} + d_{\varepsilon}(P'_P - P'_E) \quad (11)$$

$$V_n = V^*_n + d_n(P'_P - P'_N) \quad (12)$$

The computational procedure is similar to the one described by Baliga and Patankar (1983), and Gresho et al. (1984). The resulting system of the coupled equations (1-4) with the associated boundary conditions have been solved numerically using control volume based finite volume method. The computational domain consists of  $50 \times 50$  main grid points which correspond to  $50 \times 40$  U and V staggered grid points. The control volume based finite volume method provides the smooth solutions at the interior domain including the corner regions. To ensure the convergence of the numerical solution to the exact solution, the grid sizes have been optimized and the results presented here are independent of grid sizes.

Grid refinement tests have been performed for the case  $Re = 100$  and  $Gr = 1000$  using eight uniform grids  $15 \times 15$ ,  $25 \times 25$ ,  $40 \times 40$ ,  $50 \times 50$ ,  $60 \times 60$ ,  $75 \times 75$ ,  $90 \times 90$  and  $100 \times 100$ . Results show that when we change the mesh size from a grid of  $25 \times 25$  to a grid of  $50 \times 50$ , the maximum value of stream function contour ( $\psi_{max}$ ) and the maximum temperature contour ( $T_{max}$ ) undergoes an increase of only 0.5% and 0.25%, respectively; then, because of calculation cost, the  $50 \times 50$  grid is retained.

The computer code has been validated with the solutions are available in the literatures. There are some possibilities of validating the numerical code. One possibility is to compare the numerical results obtained by our code with benchmarks available in the literature according to different works. Another option is to simulate a similar problem investigated by other authors with well accepted available results.

#### 4. RESULT AND DISCUSSION

The computational domain consists of  $50 \times 50$  main grid points which correspond to  $50 \times 40$  U and V staggered grid points. Numerical solutions are obtained for various values of  $Ri = 0 - 10$ ,  $Pr = 0.01 - 10$  and  $Re = 1 - 10^2$  with uniform heating of the top wall where the two vertical walls are cooled and the two inflow opening are located at the top of the both vertical walls with a horizontal velocity,  $U=1$ , and outflow opening are located at the bottom of both vertical wall. The jump discontinuity in Dirichlet type of wall boundary conditions at the corner point (see Fig.1) corresponds to computational singularity. To ensure the convergence of the numerical solution to the exact solution, the grid sizes have been optimized and the results presented here are independent of grid sizes.

### 4.1 Characteristics of Flow Velocity

The Fig.2 (a)-(c) illustrate the velocity contours with the constant temperature heated top wall for  $Ri = 1$ ,  $Pr = 0.7$  and  $Re = 1$  to  $100$ . Fig.2 (a) show the effect of laminar flow, because it's and  $Re = 1$ . The velocity contours are distributed symmetrically about the vertical central line. In the case of inflow opening velocity contours are distributed in oval shape and outflow opening it is almost round shape. But in the case of Fig.2 (b), (c) the value of  $Re$  increases the shape of velocity contours will be changed. As the  $Re$  increases the shape of velocity contours changes due to adverse pressure gradient. Further increases in the value of  $Re$  circulating flow will be developed in the enclosure. The strength of circulation depending on values of Reynolds number and maximum exit flow occur at left corner of the bottom wall.

### 4.2 Effect of Richardson Number

Figures 3 to 5 show streamline plots for different values of  $Ri$  at  $Re = 10$  and  $Pr = 1$  to  $10$ . At low  $Ri$ , buoyancy effects are weak, and separation occurs at the opposite side of the heated surface. As  $Ri$  increases, buoyancy effects accelerated the fluid near the heated wall causing the anticlockwise circulation near the hot wall to be increased. As shown above figures, the thermal boundary layer decreases in thickness slowly as the  $Ri$  increases. Fig.3 (a) – (c) shows the stream function and temperature contours for various  $Ri$  with  $Pr = 0.1$  and  $Re = 10$ .

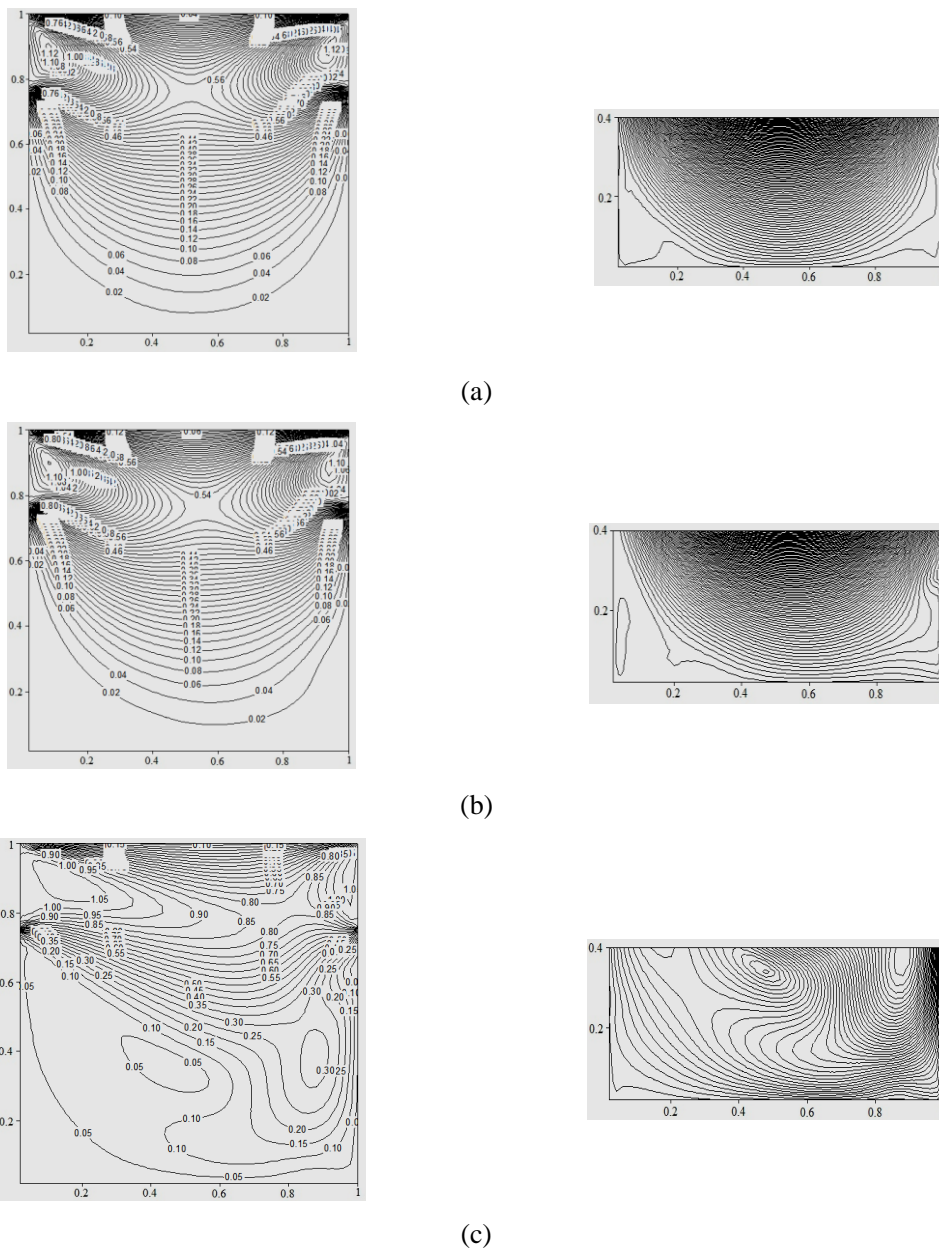


**Fig.2.** Flow velocity contours with  $Pr = 0.7$ ,  $Ri = 1$ : (a)  $Re = 1$ , (b)  $Re = 10$ , and (c)  $Re = 100$

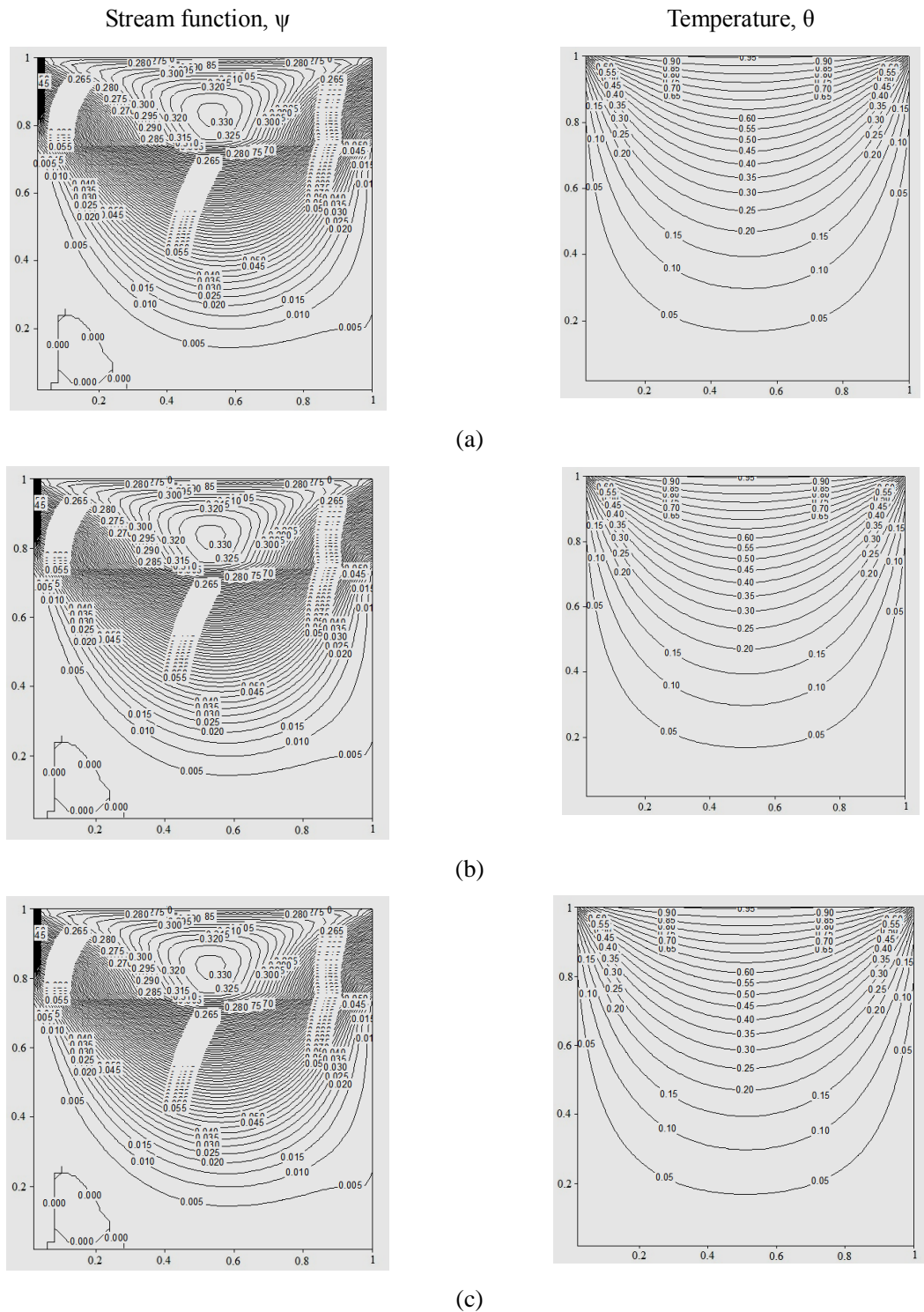


**Fig3.** Stream function and temperature contours with  $Pr = 0.7$ ,  $Re = 1$ : (a)  $Ri = 0$ , (b)  $Ri = 1$ , and (c)  $Ri = 10$

Fig.3 (a) display the effect of ventilated flow inside the enclosure for  $Ri = 0$ . It is observed that two inflow entering at top of the enclosure and it mixing inside the cavity, and circulation developed at top of the cavity. The exit opening at bottom left corner a clockwise circulation is developed because of adverse pressure gradient. At the low Prandtl number flow thickness of thermal boundary layer is greater than that of hydrodynamic boundary layer, and then the temperature contours are smooth and symmetrical with vertical center line. In the presence of adverse pressure gradient flow separate at bottom left corner, then flow will be exiting at the right bottom corner of the enclosure.

Figs.4 (a) to (c) display the effect of  $Ri$  varying within 0 to 10 and  $Pr = 0.7$ . This is similar to Fig.3 (a) to (c), at low value of Prandtl number isothermal contours are almost similar. But in the case of Fig.5 (a) to (c) value of Prandtl number increases thickness of hydrodynamic boundary layer is dominating

compared to the thermal boundary layer thickness, then thermal isotherm shifted towards top heated wall.

### 4.3 Effect of Reynolds number

Figs.6 and 7 display the stream function and isothermal contours for  $Re = 1, 10, 100$  and  $1000$  with  $Ri = 1$  corresponding to  $Pr = 0.7$  (see Fig. 6) and  $10$  (see Fig. 7) with constant temperature heating of bottom wall. The increase in  $Re$  enhances effect of forced convection and suppresses the effect of natural convection. This can also be explained based on Richardson number  $Ri$ .

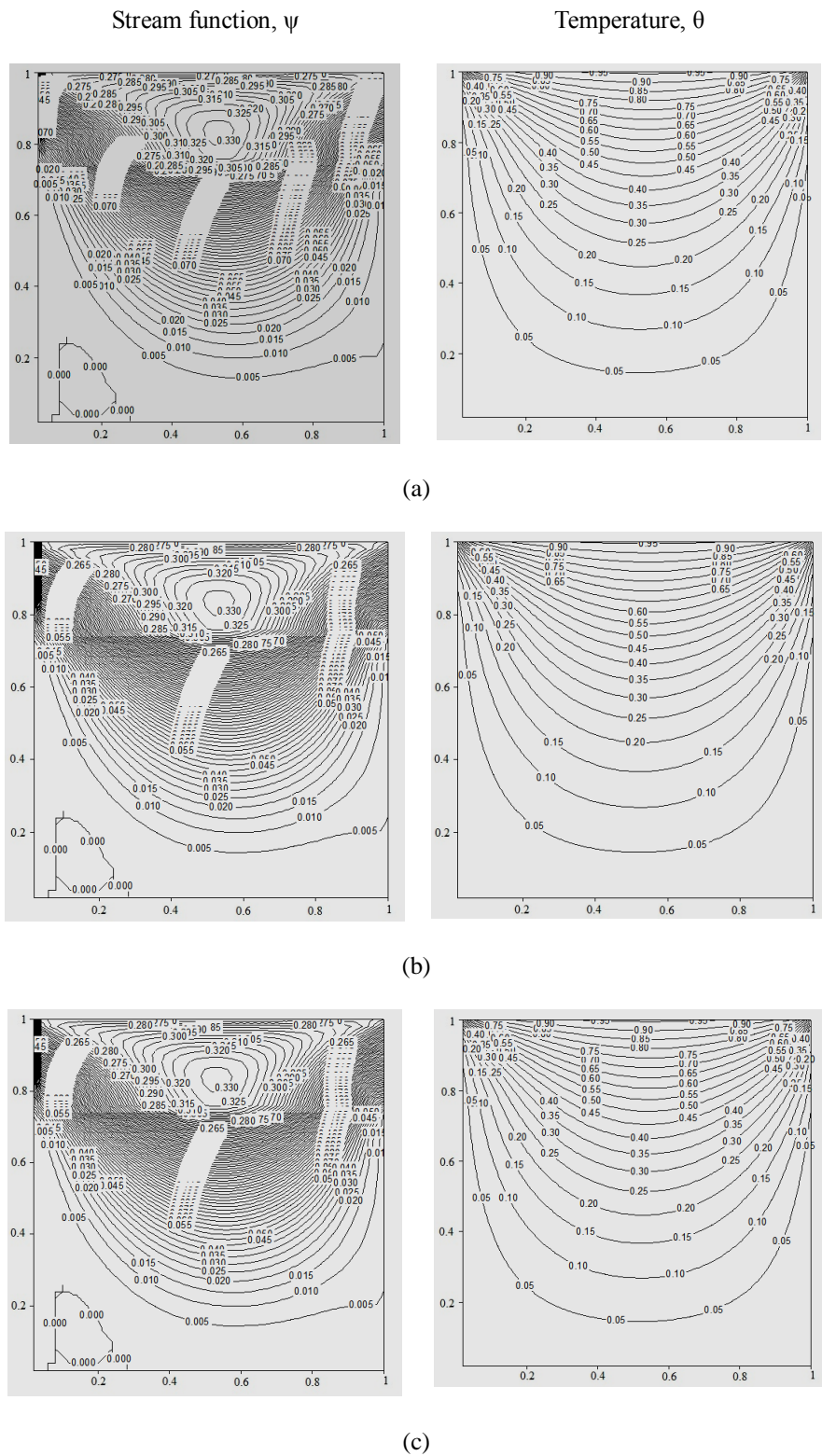
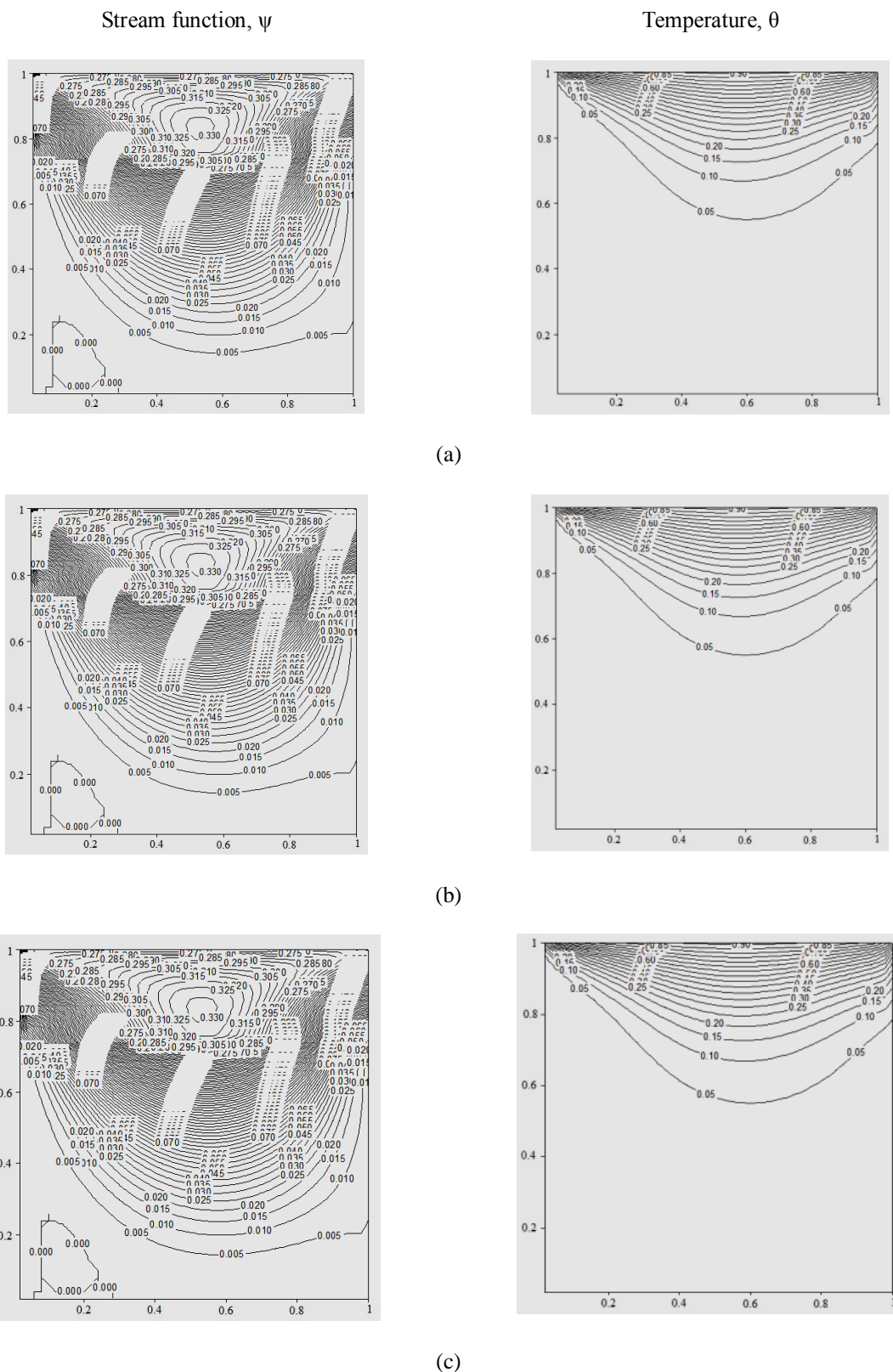


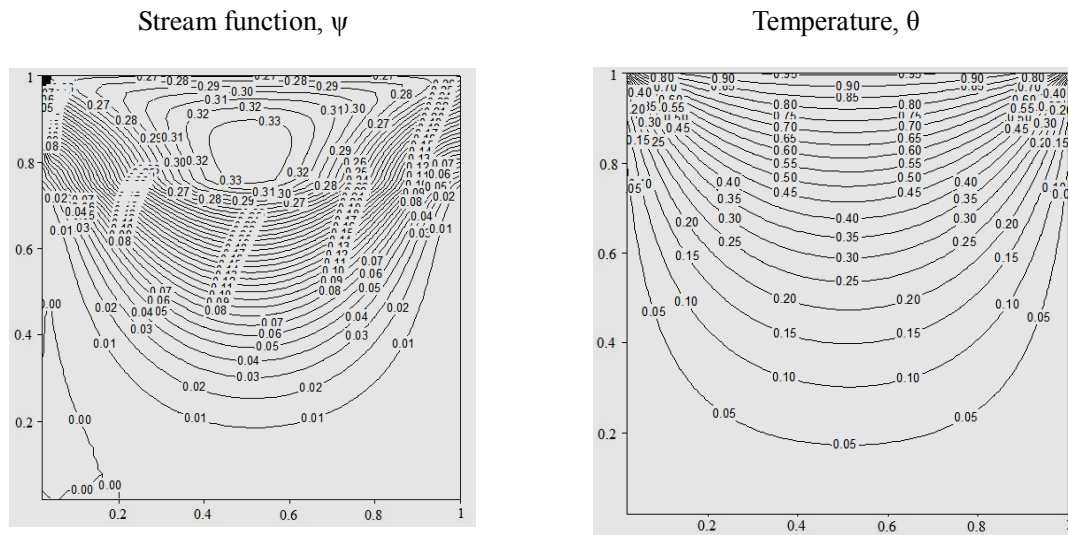
Fig4. Stream function and temperature contours with  $Pr = 1, Re = 1$ : (a)  $Ri = 0$ , (b)  $Ri = 1$ , and (c)  $Ri = 10$



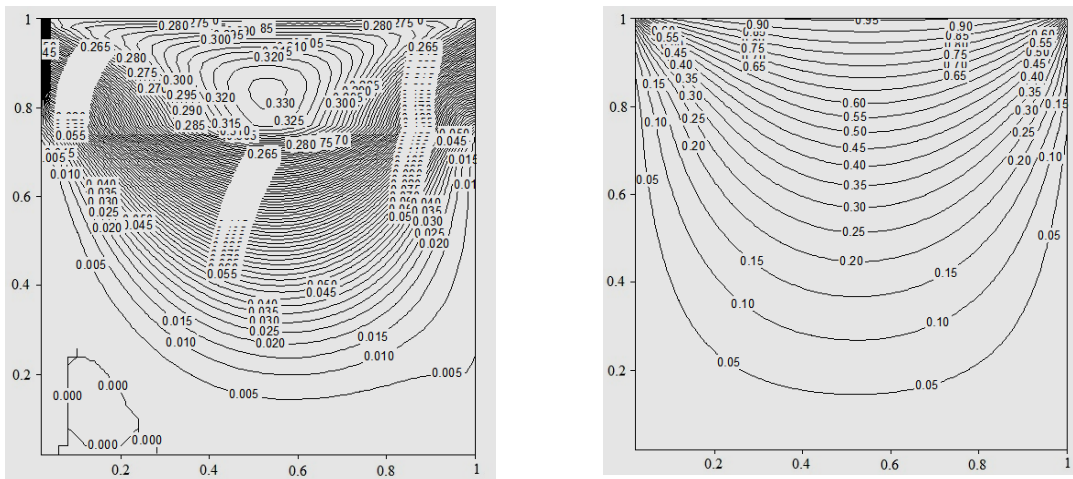
**Fig5.** Stream function and temperature contours with  $Pr = 10$ ,  $Re = 1$ : (a)  $Ri = 0$ , (b)  $Ri = 1$ , and (c)  $Ri = 10$

Fig.6 (a) to (c) shows the temperature contour for various value of  $Re$  at  $Pr = 0.7$ . It observed that low Reynolds number flow contours are smooth and symmetrical with vertical central line; this also illustrates a conduction dominated effect (see Fig.6 (a) and (b)). The value of Reynolds number increases, it is observed that a large region near the left half becomes isothermally cooled and the effect of heating will be confined only near the top and right walls of the enclosure forming a strong thermal boundary layer attached to the top wall occupying only 40% of the enclosure. Fig.7 (a) to (c) illustrate the stream function and temperature contours for  $Ri = 1$  and  $Pr = 10$  with various  $Re$  in

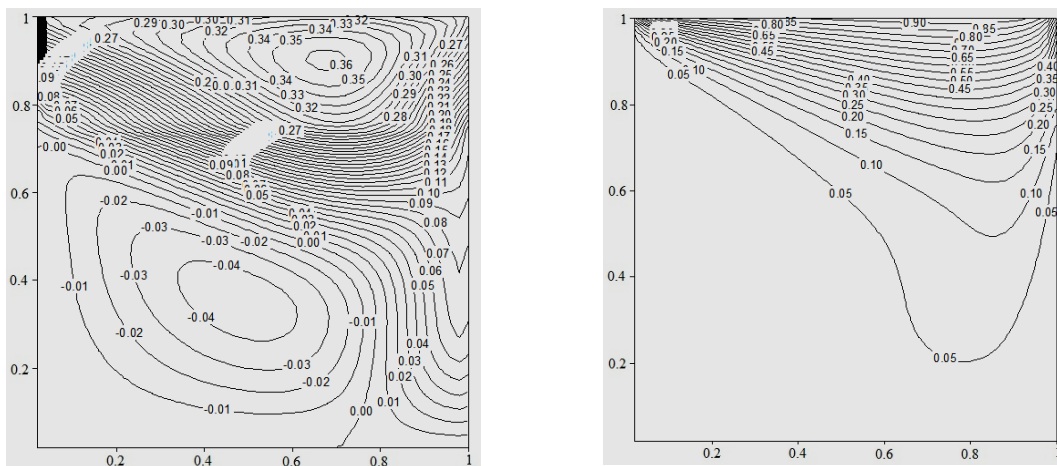
presence of uniform heating of top wall. It is observed that value of  $Re$  and  $Pr$  will be increased thermal boundary layer attached to the top wall, then about 80% of region inside the cavity is isothermally cooled.



(a)



(b)



(c)

**Fig6.** Stream function and temperature contours with  $Pr = 0.7$ ,  $Ri = 1$ : (a)  $Re = 1$ , (b)  $Re = 10$ , (c)  $Re = 10^2$

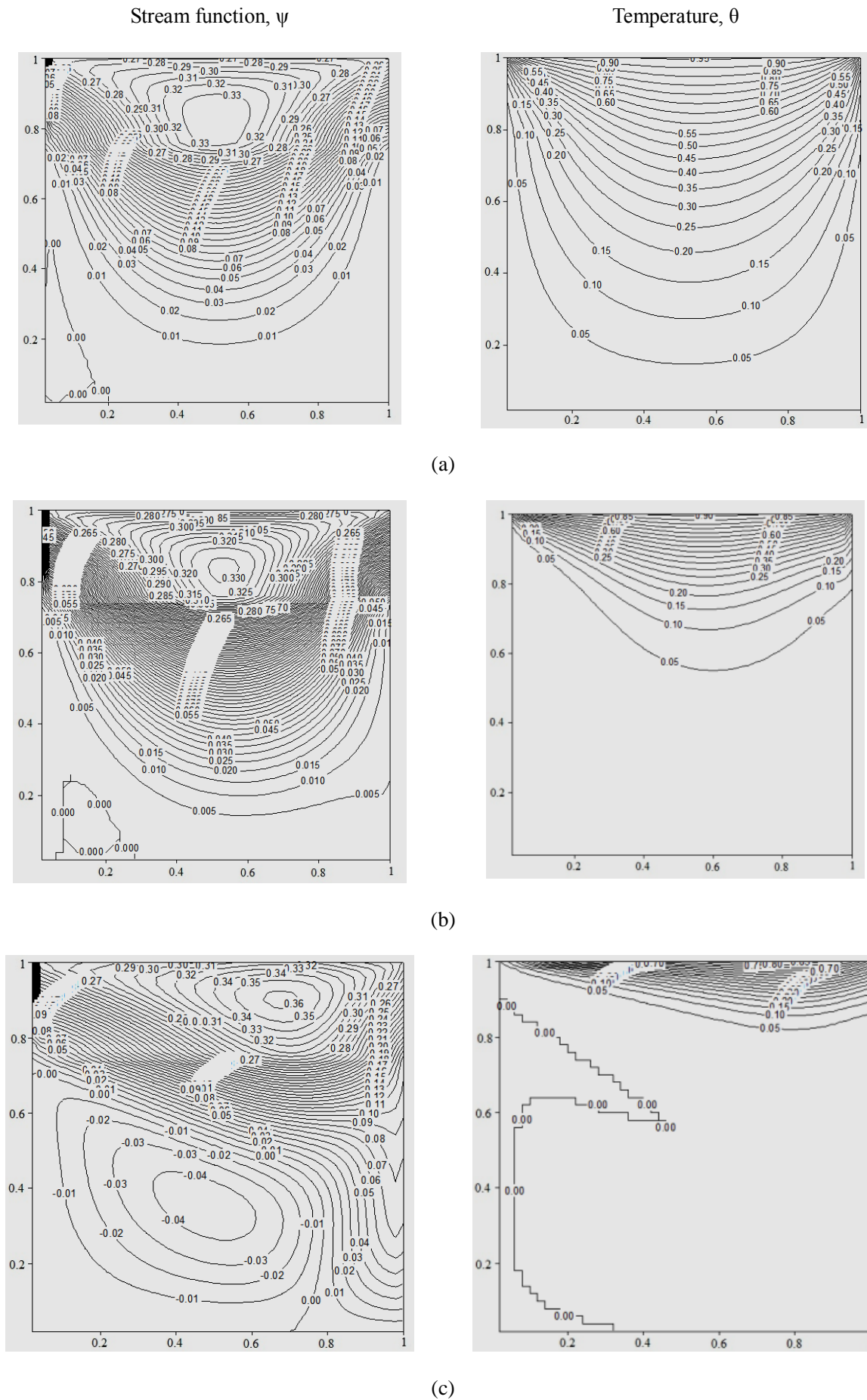


**Fig7.** Stream function and temperature contours with  $Pr = 10, Ri = 1$ : (a)  $Re = 1$ , (b)  $Re = 10$ , (c)  $Re = 10^2$

4.4 Effect of Prandtl Number

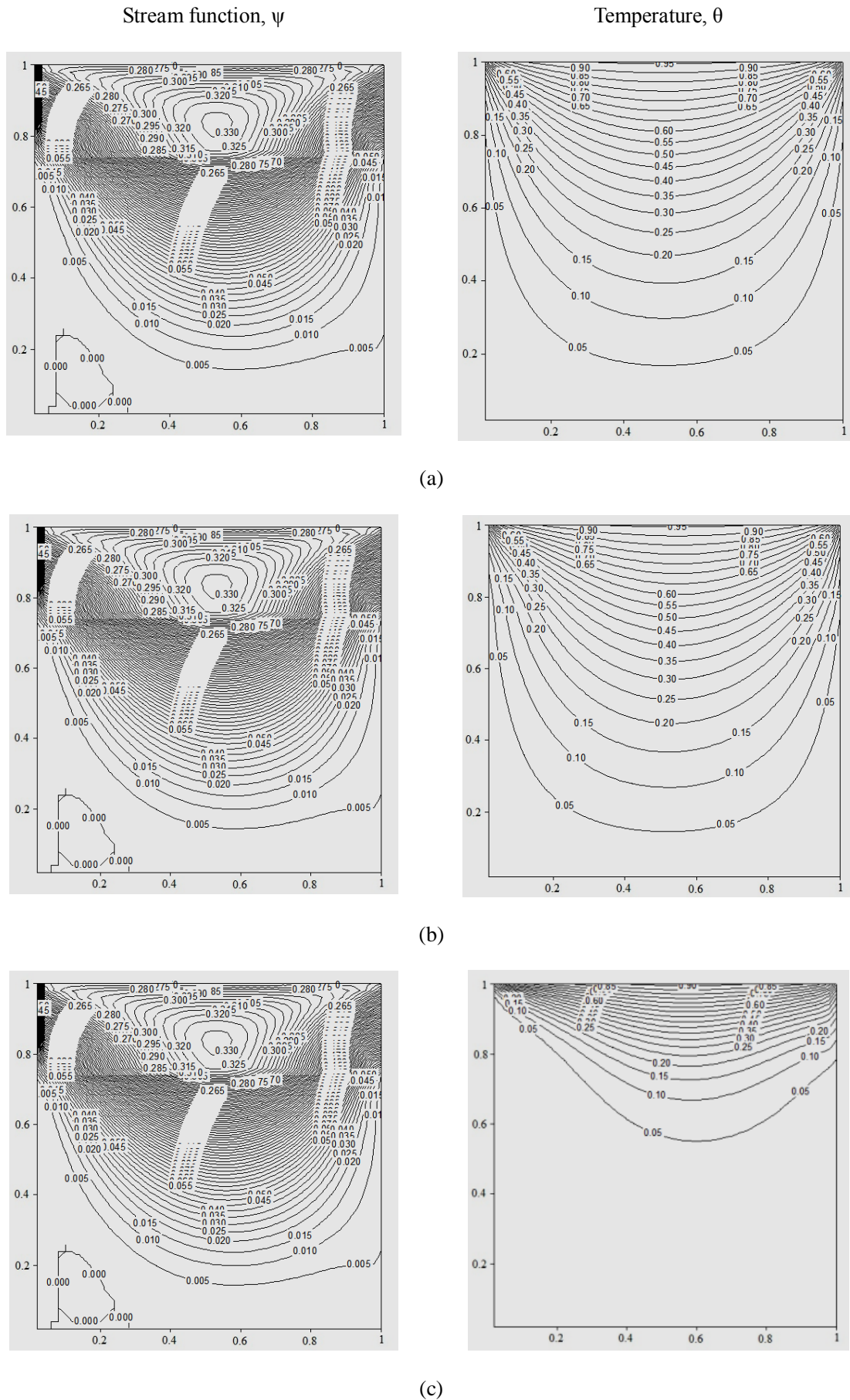
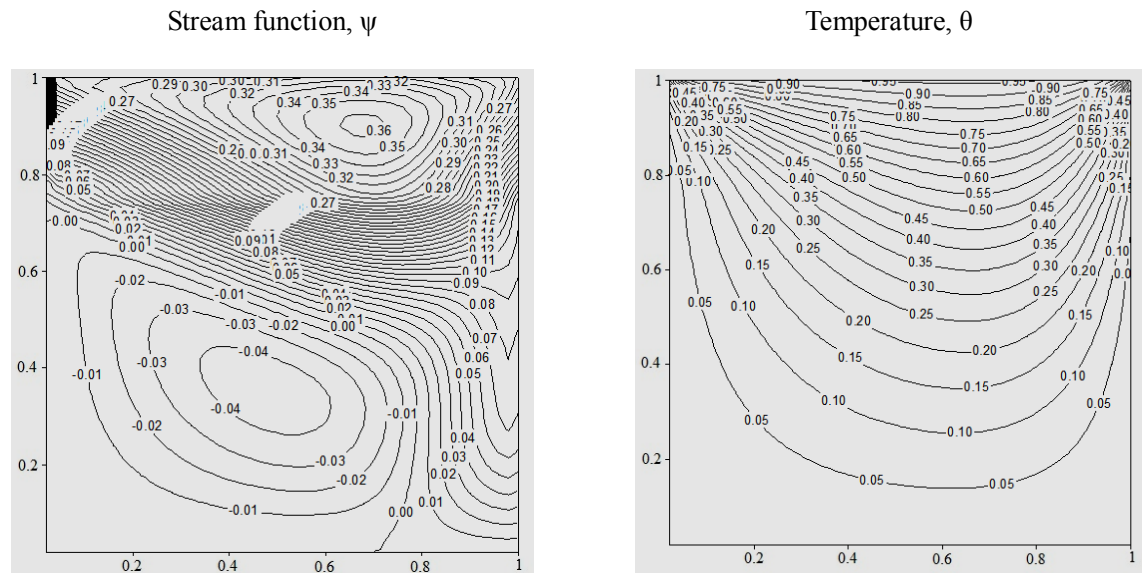
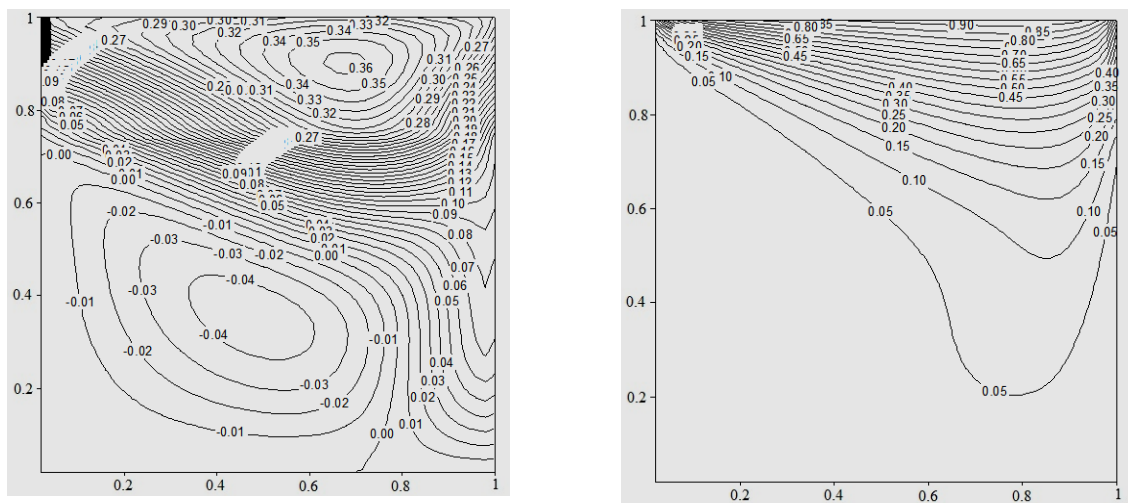


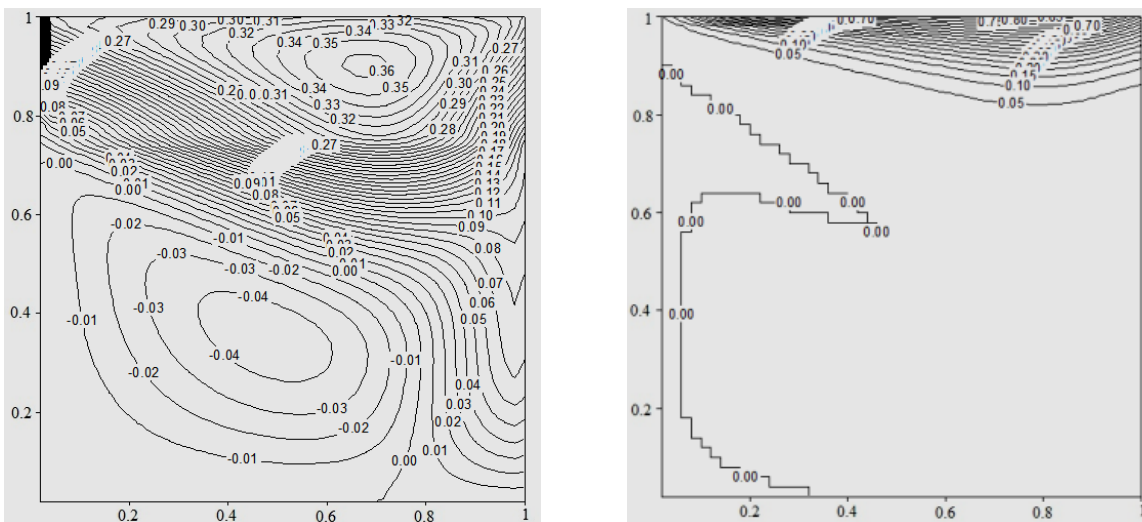
Fig8. Stream function and temperature contours with  $Re = 10, Ri = 1$  : (a)  $Pr = 0.1$ , (b)  $Pr = 0.7$ , (c)  $Pr = 1$



(a)



(b)



(c)

**Fig9.** Stream function and temperature contours with  $Re = 100$ ,  $Ri = 1$  : (a)  $Pr = 0.1$ , (b)  $Pr = 0.7$ , (c)  $Pr = 1$

Figs.8 and 9 shows the stream function and isotherm contours for  $Pr = 0.1, 0.7$  and  $10$  with  $Re = 10$  and  $100$  corresponding to  $Ri = 1$ . Fig.8 (a) to (c) display the effect of varies values of  $Pr$  with  $Re = 10$  and  $Ri = 1$ . The lower Prandtl number thermal diffusivity momentum higher that of hydrodynamic momentum diffusivity, then temperature contours are smooth and symmetrical about vertical center line (see Fig.8 (b) and (c)). This also illustrates a conduction dominated effect inside the enclosure. The heating effect is qualitatively smaller as seen in Fig.8 (c), a larger cold region developed inside the cavity. In this case all isothermal contours shifted towards the top wall. The value  $Pr$  is increased, the corresponding decrease in the fluid conductivity limits the acceleration of the near hot- wall fluid to a thinner thermal boundary layer region (seen in Fig.9 (a) to (c)).

The value of  $Pr$  increases the space of cold region will be increased. Fig.9 (c) is observed that a large region near the left half becomes isothermally cooled and the effect of heating will be confined only near the top and right walls of the cavity forming a strong thermal boundary layer attached to the top wall occupying only 10% of the cavity.

### 5. CONCLUSION

A numerical investigation on mixed convection in a ventilated enclosure with various boundary conditions was carried out using a finite volume method. The prime objective of the investigation is to study the effect of uniform heating of the top wall, on the flow and heat transfer characteristics due to mixed convection in enclosure. It is evident from Figs. 3-5 for fixed  $Re$  and  $Pr$ , the strength of circulation increases with the increase in  $Ri$ . As  $Ri$  increases, the effect of buoyancy increases leading to an increase in the strength of circulation. Due to increase in circulation strength, the isotherms are stretched along the side walls and heat is transferred mostly by convection for higher value of  $Pr$ . The effect of  $Re$  has also been studied in the present investigation for fixed value of  $Pr$  and  $Ri$ . It is observed that the effect of natural convection decreases and forced convection increases with the increase of  $Re$ . It has also been observed that for higher value of  $Pr$ , the effect of heating is more pronounced near the top and right walls as the formation of thermal boundary layers is restricted near the top and right wall for uniform heating cases. The heat transfer rate is very high at the edges of the top wall and it decreases at the center of the cavity.

Laminar convection in a two-dimensional, horizontally driven rectangular enclosure with a prescribed constant temperature heat source mounted on the top wall is simulated numerically in this work. Mixed convection arises as the buoyancy-induced cold flow from the source interacts with an externally induced cold air flow. The effects of different ventilation orientations are also described to figure out the best cooling performance. The heat transfer results explain the importance of the non-dimensional parameters like Reynolds number and Richardson number in the natural and mixed convection regime. The effects of these parameters on the flow fields are also investigated. The governing parameter affecting heat transfer is the Richardson number. For  $Ri > 1$ , the heat transfer is dominated by natural convection. When  $Ri < 1$ , the flow and heat transfer are dominated by forced convection. The mixed regime is obtained when  $Ri = 1$ .

### ACKNOWLEDGEMENT

The authors wish to acknowledge Department of Mechanical Engineering, LBS College of Engineering, Kasaragod, India, for support and technical help throughout this work.

### REFERENCES

- [1] Burggraf, O.R., Analytical and numerical studies of the structure of steady separated flows, *Journal of Fluid Mechanics*, 1966, 24, 113-151
- [2] O. Botella and R. Peyret., Benchmark spectral results on the lid-driven cavity flow, *Computers & Fluids* Vol. 27, No. 4, pp. 421-433, 1998
- [3] Charles-Henri Bruneau and Mazen Saad., The 2D lid-driven cavity problem revisited, *Computers & Fluids* 35 (2006) 326–348
- [4] Chen, Q., Mayers, C.A., Vander Kooi, J. 1989. "Convective heat transfer in rooms with mixed convection," in: *International Seminar on Indoor Air Flow Patterns*, University of Liege, Belgium. pp. 69–82.

- [5] Spitler, J.D. 1990. "An experimental investigation of air flow and convective heat transfer in enclosures having large ventilation rates," PhD Thesis, University of Illinois at Urbana-Champaign, USA.
- [6] Fisher, D.E.1995. "An experimental investigation of mixed convection heat transfer in a rectangular enclosure," PhD Thesis, University of Illinois at Urbana-Champaign, USA
- [7] Pavlovic, M. D., Penot, F. 1991. "Experiments in the mixed convection regime in an isothermal open cubic cavity," *Experimental Thermal and Fluid Science* 4, pp. 648–655.
- [8] Du, S-Q., Bilgen, E., Vasseur, P. 1998. "Mixed convection heat transfer in open ended channels with protruding heaters," *Heat Mass Transfer* 34, pp. 265–270.
- [9] Sathe, S.B., Sammakia, B.G. 2000. "A numerical study of the thermal performance of a tape ball grid array (tbga) package," *J Electronic Packaging* 122, pp. 107–114.
- [10] Harman, S.A., Cole, K.D.2001. "Conjugate heat transfer from a two layer substrate model of a convectively cooled circuit board," *J Electronic Packaging*. Vol. 123: 156–158
- [11] Thrasher, W.W., Fisher, T.S., Torrance, K.E. 2000. "Experiments on chimney-enhanced free convection from pin-fin heat sinks," *J Electronic Packaging* 122, pp. 350–355.
- [12] Jilani, G., Jayaraj, S., Voli, K.K. 2001. "Numerical analysis of free convective flows in partially open enclosure," *Heat Mass Transfer*. DOI 10.1007/ S002310100251/ online publication, Nov 29.
- [13] Ligrani, P.M., Choi, S.1996. "Mixed convection in straight and curved channels with buoyancy orthogonal to the forced flow," *Int. J. Heat Mass Transfer* Vol. 39(12): 2473-2484.
- [14] Hattori, N. 1979. "Combined free and forced convection heat transfer for fully developed laminar flow in horizontal concentric annuli (numerical analysis)," *Heat Transfer: Jpn. Res.* Vol. 8(4): 27-48.
- [15] Karki, K.C., Patankar, S.V. 1989. "Laminar mixed convection in the entrance region of a horizontal annulus," *Numer. Heat Transfer* 15, pp. 87-99.
- [16] Nonio, C., Giudice, S.D. 1996. "Finite element analysis of laminar mixed convection in the entrance region of horizontal annular ducts," *Numer. Heat Transfer, Part A* 29, pp. 313-330

#### **AUTHOR'S BIOGRAPHY**

**Robins Aikkara** doing M.Tech in Thermal and Fluids Engineering at LBS College of Engineering, Kasaragod, Kerala